

We are IntechOpen, the world's leading publisher of Open Access books Built by scientists, for scientists

6,600

Open access books available

178,000

International authors and editors

195M

Downloads

Our authors are among the

154

Countries delivered to

TOP 1%

most cited scientists

12.2%

Contributors from top 500 universities



WEB OF SCIENCE™

Selection of our books indexed in the Book Citation Index
in Web of Science™ Core Collection (BKCI)

Interested in publishing with us?
Contact book.department@intechopen.com

Numbers displayed above are based on latest data collected.
For more information visit www.intechopen.com



Chapter

Distinct Roles of the Principal Exchange-Correlation Energy and the Secondary Correlation Energy Functionals in the MGC-SDFT-UHFD Decoupling

Masami Kusunoki

Abstract

The Kohn-Sham formalism for the density functional theory (DFT) proposed a half-century ago has been the extensive motive force for the material science community, despite it is incomplete because of its problematic notion of eternally-unknown correlation energy functional including a separated part of kinetic energy. Here, we widely explain an alternative method recently discovered by us, i.e. the multiple grand canonical spin DFT (MGC-SDFT) in the unrestricted Hartree-Fock-Dirac (MGC-SDFT-UHFD) approximation. It is proved that the correlation energy functional consists of well-defined principal and secondary parts: the former yields the principal internal energy functional responsible for a set of the one-body quasi-particle spectra defined by the respective ground and excited states with each natural LCAO-MO as well as a set of the expected values of Heisenberg spin Hamiltonian, and the latter does a well-defined spin-dependent perturbation energy responsible for some many-body effects. An application will be made to explain why the water-splitting S_1 -state Mn_4CaO_5 -clusters in photosystem II can exhibit two different EPR signals, called “g4.8” and “g12-multiline”. Moreover, the *secondary correlation energy part* will be shown to promote Cooper-pairings of Bloch-electrons near Fermi level in the superconductor, provided that their eigenstates might be exactly determined by the MGC-SDFT-UHFD method.

Keywords: spin density functional theory (SDFT), LCAO-natural molecular orbitals (NMO), principal exchange-correlation energy, Heisenberg spin Hamiltonian, secondary correlation energy, superconductivity

1. Introduction

In this chapter, we aim to explain why the predominant Kohn-Sham formalism of density functional theory (KS-DFT) based on the variational principle with respect to the electron density in a closed N -electron system [1–6], must be stated as incomplete,

during a number of active works motivated on it (e.g [7–12]) still continuing, by pushing out the alternative electron density functional theory based on the multiple grand canonical quantum statistical variational principle capable of generating a large enough number of quantized energy levels of the ground and excited states in the unrestricted Hartree-Fock-Dirac approximation taking account of the explicit principal exchange-correlation energy functional $-K_{XC}$. This ultimate theory has been recently developed and called “multiple grand canonical spin DFT in the UHFD approximation (MGC-SDFT-UHFD method)” [13]. Moreover, we aim to present here a compact text of this ultimate MGC-SDFT-UHFD method in Sections 2.1 and 2.2 in order to help not only the reader’s understanding but also some program developers to challenge this painful-but-promising project to revise some codes associated with this paradigm shift from KS-DFT to MGC-SDFT-UHFD world in an extensive range of so far dedicated codes for predicting molecular and crystalline properties.

It is also important and exciting for us to be able to present as much as possible experimental evidence powerfully supporting the quantitative and systematic aspects of the MGC-SDFT-UHFD method to determine the one-body energy spectra, the quasi-particle’s wave functions, the magnetic property such as the mean isotropic spin-exchange coupling constants $\{J_{i,j}\}$ and the total electronic internal energies, in Section 2.3. In [13], we provided the first experimental evidence for it; in **Table 1**, the derived formulas for $J_{1,2}$ demonstrated excellent quantitative agreements (less than 1% errors) with 10 experimental results from biomimetic binuclear transition metal complexes (TM: Cu, Mn, Fe), using the Mulliken’s atomic spin densities [14] and a set of the internal energies calculated by the UB3LYP/PBS/lacvp** method [15, 16]. Among many controversial problems that remained to be elucidated in photosynthesis research (see a recent review [17]), in Section 2.4 we discuss the second experimental supporting evidence provided by two broad EPR signals, named “g4.8” [18, 19] and “g12-multiline” [20], observed from the dark-stable S_1 state Mn_4CaO_5 clusters in the PSII having slightly different structures between thermophilic cyanobacteria in [18, 19] and higher-plant spinach in [20], respectively. At present, however, we have at hand only the structure of former’s PSII crystal at 1.95 Å high-resolution viewed by femtosecond XFEL pulse irradiation [21] but do not have any structure of the latter PSII crystal at least at similar high-resolution. It should be also noted that the super-brilliant femtosecond XFEL-pulse irradiation may generate high-density secondary photoelectrons to deoxidize nearby Mn_4 clusters with high probability during diffraction measurements. Then, the quantitative determination of the Heisenberg spin Hamiltonian involved in *the principal exchange-correlation energy function* can play a key role in the geometry optimization by the UB3LYP/PBS(ϵ)/lacvp** method to make the model Mn_4CaO_x cluster being thermally distributed in some isomeric substates of any Kok- S_i state.

Furthermore, in Section 2.5, we discuss the most interesting many-body effect induced by the *secondary correlation energy term*, which represents a spin-dependent attractive correlation interaction between a couple of conductive Bloch-electrons with antiparallel spins that could be generated only near the Fermi surface in the metallic crystal. This strong correlation interaction may accelerate the phase transition from the normal state to the superconductive state by promoting Cooper-pairings of conductive Bloch-electrons near the Fermi level in the superconductor against the common knowledge [22–27].

A problematic idea underlining the KS-DFT formalism may be described in other words such that the ground state energy E of the one-particle self-consistent field Hamiltonian for N electron systems, which corresponds to the internal energy functional of the electron density determined in thermal equilibrium state, should be further

Complexes	a Cu ₂ ^{II,II}	c Mn ₂ ^{IV,IV}	d Mn ₂ ^{III,IV}	e Mn ₂ ^{III,IV}	f Mn ₂ ^{IV,III}	g Mn ₂ ^{IV,IV}	h Mn ₂ ^{II,II}	i Fe ₂ ^{II,II}	j Mn ₂ ^{III,III}	k Fe ₂ ^{III,III}
N_A	62	118	91	89	86	88	77	77	81	81
$R_{1,2}(\text{\AA})$	2.659	2.745	2.591	2.591	3.230	2.296	3.370	3.315	3.140	3.202
bridge ligands	(μ -OAc) ₄	(μ -O) ₂	(μ -O) ₂ (μ -OAc)	(μ -O) ₂ (μ -OAc)	(μ -O) ₂ (μ -OAc)	(μ -O) ₃	(μ -OH) ₂ (μ -OAc) ₂	(μ -OH) ₂ (μ -OAc) ₂	(μ -OH) ₂ (μ -OAc) ₂	(μ -OH) ₂ (μ -OAc) ₂
ϵ	10	20	20	20	40	20	40	20	20	10
$\Delta U_{UHFD}^{(2)} (\text{cm}^{-1})$	-271.1	-1366.	-1579.	-1549.	-506.6	-3928.	-248.9	-223.8	141.4	-2522.
$n_{1EF}^{(1)}$	0.975	3.064	4.040	4.087	3.140	3.106	4.939	3.913	4.006	4.686
$n_{1EF}^{(2)}$	0.980	3.033	4.031	4.111	-3.22	3.038	4.912	3.907	3.882	4.583
$n_{2EF}^{(1)}$	0.976	3.107	3.076	3.034	4.010	3.103	4.941	3.912	4.006	4.683
$n_{2EF}^{(2)}$	-0.981	-3.039	-3.189	-3.187	4.010	-3.026	-4.911	-3.907	-3.886	-4.636
$S_{1EF,2EF}^{(1)}$	5.13	-5.46	-3.15	-5.47	-3.74	-6.61	2.44	4.52	0.280	13.94
$S_{1EF,2EF}^{(2)}$ ($\times 10^{-2}$)	-3.76	2.38	5.50	8.21	5.69	2.13	-3.65	-4.80	-6.06	16.46
$J_{1,2}^{(4-0)}$ (cm^{-1})	-284.9	-143.5	-126.5	-123.4	-40.1	-407.6	-10.2	-14.6	8.8	-114.9
$J_{1,2}^{exp}$ (cm^{-1})	-285	-144	-125	-125	-40	-407	-9	-14	9	-115

Table 1.

Benchmark-test results of the 2GC-UHFD-SD averaged ES-exchange coupling constants, designated $J_{1,2}^{(4-0)}$, for 10 biomimetic binuclear Cu, Mn and Fe complexes, using the UB3LYP/PBS(ϵ)/lacvp** (4th XC) method combined with the inherent formulas of Eqs. (103), (113), derived in the present MGC-UHFD-SDFT (0th XC) method. These model TM₂ complexes consist of N_A atoms, are imbedded in each ϵ dielectric constant medium, and exhibit a variety of TM₁-TM₂ distances, designated $R_{1, 2}$, which depend strongly on different bridge structures and the different TM valences, and also weakly on the different non-bridging ligations of paramagnetically-polarized O atoms and diamagnetically-/paramagnetically-polarized N atoms (not shown here). Here the data for **b** (di- μ -oxo bridged Mn^{IV}-Mn^{IV} dimer ligated by four picolinic anions) in **Table I** in [13] was omitted because of its optimized structure containing no solvent molecules. (see Supplemental Online Material of Ref. [13] about how to calculate the effective spin densities using the Mulliken's atomic spin densities [14].)

minimized by “the *exact* variation principle” with respect to the electron density regarded as a variational variable to search for “the *exact* energy functional” of “the *exact* electron density”, subjected to the N -representability condition [4]. This wrong variational idea appears to have been widely accepted so far, although it may have been enforced by a special situation enforced by too strong expressions involving many *exact*’s: “the *exact* variational principle”, and “the existence theorem of an *exact* energy functional of the *exact* electron density” as well as “ N -representability condition”. Especially, “the N -representability condition” seems to be too strong to consider any open quantum system, in which the total numbers (N_α, N_β) of (up, down) electrons in the system should be replaced by the mean values ($\bar{N}_\alpha, \bar{N}_\beta$) of a pair of the expected values of their operators, ($\hat{N}_\alpha, \hat{N}_\alpha$), respectively, in the context of applying the variational principle to the minimum grand potential including them, as will be shown in this chapter. So far, neither theoretical proof nor evidence for the K-S formalism could not be provided unless the *exact* correlation energy function is discovered.

In a GC ensemble, one may consider a much larger M -electron system ($M \gg N$) of atoms, molecules, and solids, which will be maximally realized with a finite probability in contact with a grand canonical heat/particle reservoir containing a much larger number of electrons at temperature θ/k_B (k_B is the Boltzmann constant). All the stationary states of the M -electron system, which involve the ground and all kinds of excited states, may be assumed to be describable in terms of the time-independent non-relativistic Schrödinger wave equation in 3D-space:

$$H\Psi = E\Psi(\mathbf{x}_1, \mathbf{x}_2, \dots, \mathbf{x}_M); M \gg N, \quad (1)$$

where H is the Hamiltonian operator given by

$$H = T + V_{ne} + V_{ee}, \quad (2)$$

$$= \sum_{i=1}^M \left(-\frac{1}{2} \nabla_i^2 \right) + \sum_{i=1}^M v(\mathbf{r}_i, \varepsilon) + \sum_{i < j}^M \frac{1}{r_{ij}}. \quad (3)$$

Here, $\mathbf{x}_i \equiv (\mathbf{r}_i, s_i)$ represents the (orbital, spin) coordinates of the i th electron, T is the electron kinetic energy operator; V_{ne} is the electrostatic interaction operator of electrons with all nuclei and the surrounding medium of the dielectric constant ε if a convenient “the linear Poisson-Boltzmann equation Solver (PBS)” model [8] is augmented; V_{ee} is the electron Coulomb interaction operator; and $r_{ij} \equiv |\mathbf{r}_i - \mathbf{r}_j|$. Since it is impossible to exactly solve Eq. (1) except for the case of a hydrogen atom, we have developed the ultimate MGC-SDFT formalism [7], which has been constructed by developing five new methodological concepts in Subsections 2.1 through 2.5 along the basic principles of quantum thermodynamics with the theory of open quantum systems, but not of closed quantum system as adopted in the Kohn-Sham formalism.

2. Multiple grand canonical spin density functional theory

2.1 Definition of a grand canonical ensemble: One-particle and two-particle reduced density matrices

The principally most general choice would be made for an *extended* antisymmetric Slater determinant wave function as the trial many-electron wave function $\Psi(\mathbf{x}_1,$

$\mathbf{x}_2, \dots, \mathbf{x}_M$) in the Schrödinger Eq. (1), consisting of a complete large enough number, (M_α, M_β) , of mutually-independent *natural molecular spin-orbitals* (NMO) wave functions, Eq. (6), which may be most-appropriately expandable in terms of a Linear Combination of gaussian-type or Slater-type Atomic Orbitals (LCAO), $\mathbf{G}_A \equiv [g_l^a(\mathbf{r})]$ (a , the atomic order number from 1 to N_A ; l , a set of plural AO quantum numbers). The maximum size of (M_α, M_β) -dimensional Hilbert space of the NMO set \mathbf{M}' of Eq. (4) must be as large enough as possible to satisfy the near-completeness condition of Eq. (5) and the orthonormality relations of Eqs. (6) and (7) as far as the highest NMO energy levels may not exceed a dissociation limit given by a work function, W .

$$\mathbf{M}' = {}^\alpha \mathbf{M}' + {}^\beta \mathbf{M}' \equiv \{\Psi'_\tau(\mathbf{x}), \epsilon'_\tau; \tau = 1_\alpha, \dots, M_\alpha, 1_\beta, \dots, M_\beta\}, \quad (4)$$

$$\sum_{m\sigma}^{\sigma \mathbf{M}'} |\Psi'_{m\sigma}\rangle \langle \Psi'_{m\sigma}| \cong \mathbf{1} \text{ for } M_\sigma \gg N_\sigma; \sigma = \alpha, \beta. \quad (5)$$

$$\Psi'_{m\sigma}(\mathbf{x}) \equiv \Phi'_{m\sigma}(\mathbf{r}) \xi'_{m\sigma}(\mathbf{s}), \quad (6)$$

$$\langle \Psi'_{m\sigma} | \Psi'_{m'\sigma'} \rangle = \langle \Phi'_{m\sigma} | \Phi'_{m'\sigma'} \rangle \langle \xi'_{m\sigma} | \xi'_{m'\sigma'} \rangle = \delta_{m\sigma, m'\sigma'} \delta_{\sigma, \sigma'}, \quad (7)$$

$$\Phi_{m\sigma}(\mathbf{r}) = \sum_{a,l}^{\mathbf{G}_A} C_{a,l}^{m\sigma} g_l^a(\mathbf{r}) = \sum_{a=1}^{N_A} \sum_{l} C_{a,l}^{m\sigma} g_l^a(\mathbf{r}). \quad (8)$$

In Eq. (8), the AO basis functions, which may include polarization and diffuse functions, are assumed to be orthonormalized in each atom such as $\langle g_l^a | g_{l'}^a \rangle = \delta_{l,l'}$ but slightly overlap between the valence-electron orbitals of neighboring atoms, except for most AOs in the core levels. Hereafter, the single dashed quantities in Eqs. (4)–(7) will be used for the quantities in a thermal nonequilibrium state. The completeness Eq. (5) and the orthonormality Eqs. (6) and (7) are assumed to seamlessly hold even in such non-equilibrium states.

It is important to remind that the thermodynamic equilibrium state can be achieved in terms of the Rayleigh-Ritz variational principle applied to the one-particle reduced density matrix given by

$$\widehat{\Gamma}[p', \Psi'] \equiv \sum_{N'}^{\infty} \sum_{\tau}^{\mathbf{M}'} P'_{N',\tau} |\Psi'_{N',\tau}\rangle \langle \Psi'_{N',\tau}|, \quad (9)$$

$$= \sum_{\tau}^{\mathbf{M}'} \sum_{n_\tau=0}^1 p'_{\tau, n_\tau} |\Psi'_{\tau, n_\tau}\rangle \langle \Psi'_{\tau, n_\tau}|, \quad (10)$$

with respect to a set of the distribution probabilities, designated $\{P'_{N',\tau}; N' = 0, \dots, \infty; \tau = 1, \dots, M\}$ for fermions and bosons in Eq. (9) or $\{p'_{\tau, n_\tau}; \tau = 1, \dots, M; n_\tau = 0, 1\}$ for (NMO-transformed) fermions in Eq. (10). This nonequilibrium state will relax to the maximum entropy state keeping the normalization condition of Eq. (11) and the binary chemical potential (μ_α/μ_β) equilibrium conditions with the heat/particle reservoir leading to Eqs. (12) and (13):

$$\text{Tr}[\widehat{\Gamma}] = \sum_{\tau}^{\mathbf{M}'} \sum_{n_\tau=0}^1 p'_{\tau, n_\tau} = 1, \quad (11)$$

$$\hat{N}_\sigma = \sum_{\tau(\sigma)}^{\sigma M'} \hat{a}_{\tau(\sigma)}^\dagger \hat{a}_{\tau(\sigma)}; \sigma = \alpha, \beta \quad (12)$$

$$\text{Tr} \left[\hat{N}_\sigma \hat{\Gamma} \right] = \sum_{\tau(\sigma)}^{\sigma M'} \sum_{n_{\tau(\sigma)}=0}^1 n_{\tau(\sigma)} p'_{\tau(\sigma), n_{\tau(\sigma)}} \equiv \bar{N}_\sigma [p', \Psi'], \quad (13)$$

where \hat{a}_τ and \hat{a}_τ^\dagger are the annihilation and creation operators of an electron in the τ th NMO-eigenstate, respectively. Subsequently, using the GC entropy

$$\Sigma[p', \Psi'] = -k_B \text{Tr} \left(\hat{\Gamma} \ln \hat{\Gamma} \right) = -k_B \sum_{\tau}^M \sum_{n_\tau=0}^1 p'_{\tau, n_\tau} \ln p'_{\tau, n_\tau}, \quad (14)$$

and the second quantization expression of the Hamiltonian operator, that is

$$\hat{H} = \hat{H}_0 + \hat{H}_1 = \sum_{\tau}^M \epsilon'_\tau \hat{a}_\tau^\dagger \hat{a}_\tau + \hat{H}_1, \quad (15)$$

which in general consists of the principal part \hat{H}_0 and the secondary part \hat{H}_1 , responsible for the GC ensemble of mutually independent NMO fermions and a perturbational interaction between them, respectively, we obtain the grand potential in thermal nonequilibrium state:

$$\Omega[p', \Psi'] \equiv \text{Tr} \left[\hat{\Gamma} \left(\theta \ln \hat{\Gamma} + \hat{H}_0 - \mu_\alpha \hat{N}_\alpha - \mu_\beta \hat{N}_\beta \right) \right], \quad (16)$$

$$= \sum_{\tau}^M \sum_{n_\tau=0}^1 p'_{\tau, n_\tau} \left[\theta \ln p'_{\tau, n_\tau} + \langle \Psi'_{\tau}, n_\tau | (\epsilon'_\tau - \mu_{\sigma(\tau)}) n_\tau | \Psi'_{\tau}, n_\tau \rangle \right]. \quad (17)$$

In Eqs. (16) and (17) should be noted that \hat{H} is replaced by the principal part $\hat{H}_0 = \sum_{\tau}^M \epsilon'_\tau \hat{a}_\tau^\dagger \hat{a}_\tau$. The variational equations subject to the normalization condition Eq. (11) are given by

$$\frac{\partial}{\partial p'_{\tau, n_\tau}} \left(\Omega[\{p'_{\tau, n_\tau}, \Psi'_{\tau}\}] + \lambda \left[\sum_{\tau}^M \sum_{n_\tau=0}^1 p'_{\tau, n_\tau} - 1 \right] \right) = 0, \quad (18)$$

with λ being a Lagrange's multiplier, satisfying

$$e^{-1-\lambda/\theta} = \sum_{\tau}^M \sum_{n_\tau=0}^1 \langle \Psi'_{\tau}, n_\tau | \epsilon'_\tau - \mu_\alpha \bar{N}_\alpha - \mu_\beta \bar{N}_\beta | \Psi'_{\tau}, n_\tau \rangle. \quad (19)$$

Thus, we obtain an intermediate solution with fixed $\{\Psi'_{\tau}\}$:

$$p'_{\tau, n_\tau} \xrightarrow{\text{yields}} p_{\tau, n_\tau}^0(\Psi') = \frac{\exp \left[\langle \Psi'_{\tau}, n_\tau | (\mu_{\sigma(\tau)} - \epsilon'_\tau) n_\tau | \Psi'_{\tau}, n_\tau \rangle / \theta \right]}{\sum_{n_\tau=0}^1 \exp \left[\langle \Psi'_{\tau}, n_\tau | (\mu_{\sigma(\tau)} - \epsilon'_\tau) n_\tau | \Psi'_{\tau}, n_\tau \rangle / \theta \right]} \quad (20)$$

$$\hat{\Gamma}^0(\Psi') = \sum_{\tau} \sum_{n_{\tau}=0}^{M'} p_{\tau, n_{\tau}}^0(\Psi') |\Psi'_{\tau, n_{\tau}}\rangle \langle \Psi'_{\tau, n_{\tau}}|. \quad (21)$$

Then, the GC potential decreases by the non-negative quantity (the equality appears when $p' = p^0$), namely

$$\begin{aligned} & \Omega[\{p'_{\tau, n_{\tau}}, \Psi'_{\tau}\}] - \Omega[\{p^0_{\tau, n_{\tau}}, \Psi'_{\tau}\}] \\ &= \sum_{\tau} \sum_{n_{\tau}=0}^M p'_{\tau, n_{\tau}} \left(\theta \ln p'_{\tau, n_{\tau}} + \langle \Psi'_{\tau}, n_{\tau} | (\epsilon'_{\tau} - \mu_{\sigma(\tau)}) n_{\tau} | \Psi'_{\tau}, n_{\tau} \rangle \right) \\ & + \theta \ln \sum_{\tau} \sum_{n_{\tau}=0}^M \exp \left[\langle \Psi'_{\tau}, n_{\tau} | (\mu_{\sigma(\tau)} - \epsilon'_{\tau}) n_{\tau} | \Psi'_{\tau}, n_{\tau} \rangle / \theta \right] \\ &= \theta \sum_{\tau} \sum_{n_{\tau}=0}^M p'_{\tau, n_{\tau}} \left[\ln p'_{\tau, n_{\tau}} - \ln p^0_{\tau, n_{\tau}}(\Psi') \right] \geq 0, \end{aligned} \quad (22)$$

which is notably induced only by the increase of the GC entropy $\Sigma [p', \Psi'] - \Sigma [p^0, \Psi']$. This initial-guess state of the GC ensemble $\mathbf{M}' = \{\Psi'_{\tau}, \epsilon'_{\tau}\}$ will relax to converge toward the self-consistent, orthonormal and complete eigenvectors/eigenvalues set \mathbf{M} of Eqs. (23)–(27) by iteration technique, which will be described in Section 2.2.

$$\mathbf{M} = {}^{\alpha} \mathbf{M} + {}^{\beta} \mathbf{M} \equiv \{ \Psi_{m\sigma}(\mathbf{x}), \epsilon_{m\sigma}, f_{m\sigma}(\mu_{\sigma}); m\sigma \equiv \tau = 1_{\alpha}, \dots, M_{\alpha}, 1_{\beta}, \dots, M_{\beta} \}, \quad (23)$$

$$\sum_{m\sigma}^{\sigma \mathbf{M}} |\Psi_{m\sigma}\rangle \langle \Psi_{m\sigma}| \cong \mathbf{1} \text{ for } M_{\sigma} \gg N_{\sigma}; \sigma = \alpha, \beta. \quad (24)$$

$$\Psi_{m\sigma}(\mathbf{x}) \equiv \Phi_{m\sigma}(\mathbf{r}) \xi_{m\sigma}(\mathbf{s}), \quad (25)$$

$$\langle \Psi_{m\sigma} | \Psi_{m'\sigma'} \rangle = \langle \Phi_{m\sigma} | \Phi_{m'\sigma'} \rangle \langle \xi_{m\sigma} | \xi_{m'\sigma'} \rangle = \delta_{m\sigma, m'\sigma'} \delta_{\sigma, \sigma'}, \quad (26)$$

$$f_{m\sigma}(\mu_{\sigma}) = p_{m\sigma, 1} = \{ \exp[(\epsilon_{m\sigma} - \mu_{\sigma}) / \theta] + 1 \}^{-1} \equiv f(\epsilon_{m\sigma} - \mu_{\sigma}), \quad (27)$$

where it should be noted that only the populated distribution probability $p^0_{m\sigma, 1}$ of Eq. (20) converges to the Fermi-Dirac distribution probability $f_{m\sigma}(\mu_{\sigma})$ of Eq. (27).

Next, we need to introduce the first-order (for one-particle interactions) and the second order (for two-particle interactions) reduced electron density matrixes, $\Gamma(\mathbf{x}, \mathbf{x}')$ and $\Gamma_2(\mathbf{x}_1 \mathbf{x}_2, \mathbf{x}'_1 \mathbf{x}'_2)$, respectively, for the GC ensemble \mathbf{M} in thermal equilibrium state, as given by

$$\Gamma(\mathbf{x}, \mathbf{x}') = \sum_{\tau} f_{\tau} |\Psi_{\tau}(\mathbf{x})\rangle \langle \Psi_{\tau}(\mathbf{x}')|, \quad (28)$$

$$\Gamma_2(\mathbf{x}_1 \mathbf{x}_2, \mathbf{x}'_1 \mathbf{x}'_2) = \frac{1}{2} [\Gamma(\mathbf{x}_1, \mathbf{x}'_1) \Gamma(\mathbf{x}_2, \mathbf{x}'_2) - \Gamma(\mathbf{x}_1, \mathbf{x}'_2) \Gamma(\mathbf{x}_2, \mathbf{x}'_1)], \quad (29)$$

which will be used in Section 2.2.

2.2 The self-consistent field method in the UHFD approximation

Here, we derive the self-consistent field (SCF) method to generate such a realistic GC ensemble, \mathbf{M} , as given by Eqs. (23)–(27), in which all NMO levels will be partially occupied with the Fermi-Dirac distribution probability $f(\epsilon_{m\sigma} - \mu_\sigma)$ constrained by the chemical potentials μ_σ defined by either Eq. (27) or the Gibbs free energy per a σ -spin electron for $\sigma = (\alpha, \beta)$, as given by Eq. (30), using the mean number of σ -spin NMO-fermions for $\sigma = (\alpha, \beta)$ in Eq. (31):

$$G = \mu_\alpha \bar{N}_\alpha + \mu_\beta \bar{N}_\beta, \quad (30)$$

$$\bar{N}_\sigma = \sum_{m\sigma}^{\sigma\mathbf{M}} f(\epsilon_{m\sigma} - \mu_\sigma). \quad (31)$$

At first, we define various spinless electron density matrixes for later usage:

$$\rho_\sigma(\mathbf{r}, \mathbf{r}') = \text{Tr}_s[\Gamma_\sigma(\mathbf{x}, \mathbf{x}')]_{s=s'} = \sum_{m\sigma}^{\sigma\mathbf{M}} f_{m\sigma}(\mu_\sigma) \Phi_{m\sigma}(\mathbf{r}) \Phi_{m\sigma}^*(\mathbf{r}'); \sigma = \alpha, \beta, \quad (32)$$

$$\rho(\mathbf{r}, \mathbf{r}') = \rho_\alpha(\mathbf{r}, \mathbf{r}') + \rho_\beta(\mathbf{r}, \mathbf{r}'), \quad (33)$$

$$\rho_\sigma(\mathbf{r}) \equiv \rho_\sigma(\mathbf{r}, \mathbf{r}), \rho(\mathbf{r}) = \rho_\alpha(\mathbf{r}) + \rho_\beta(\mathbf{r}), \quad (34)$$

where Tr_s represents the trace on the spin coordinate s .

Next, we will prove that the internal energy $U[\Gamma_\alpha, \Gamma_\beta]$ as a function of the reduced density matrix $\Gamma = (\Gamma_\alpha, \Gamma_\beta)$ can be decoupled into two parts, as seen in Eq. (36): (1) the principal part $U_{UHFD}^0[\Gamma_\alpha, \Gamma_\beta]$ of Eq. (37) including the principal exchange-correlation energy functional $-K_{XC}[\rho_\alpha, \rho_\beta]$ defined by Eq. (40) and (2) a secondary part containing only a spin-dependent correlation energy functional $\Delta E_{UHFD}^{corr}[\Gamma_\alpha, \Gamma_\beta]$ defined by Eq. (43). This ultimate decoupling scheme neglecting the secondary correlation term $\Delta E_{UHFD}^{corr}[\Gamma_\alpha, \Gamma_\beta]$ of Eq. (43) will be tentatively called “the *Unrestricted Hartree-Fock-Dirac (UHFD) approximation*”. because the Dirac’s spin permutation operator (σ_i is called spinor)

$$P_{12}^\sigma = \frac{1}{2}[1 + (\sigma_1, \sigma_2)] = \frac{1}{2}[1 + 4(\mathbf{s}_1, \mathbf{s}_2)], \quad (35)$$

including an inner product of two of Pauli’s spin operators $(\sigma_1, \sigma_2) = (2\mathbf{s}_1, 2\mathbf{s}_2)$, has played a decisive role in our discovery of this new decoupling scheme. This is indeed a revolutionary discovery a long way beyond the early Unrestricted Hartree (UH), Unrestricted Hartree-Fock (UHF) and Unrestricted Hartree-Fock-Slater (UHFS) approximations. This new UHFD decoupling scheme leads to a group of fundamental equations:

$$U[\Gamma_\alpha, \Gamma_\beta] = U_{UHFD}^0[\Gamma_\alpha, \Gamma_\beta] + \Delta E_{UHFD}^{corr}[\Gamma_\alpha, \Gamma_\beta], \quad (36)$$

$$U_{UHFD}^0[\Gamma_\alpha, \Gamma_\beta] \equiv T[\rho] + V_{ne}[\rho] + J[\rho] - \frac{1}{2}K_{XC}[\rho_\alpha, \rho_\beta] + H_{ES}[\Gamma_\alpha, \Gamma_\beta], \quad (37)$$

$$V_{ne}[\rho] = \int d\mathbf{r} v(\mathbf{r}, \epsilon) \rho(\mathbf{r}), \quad (38)$$

$$J[\rho] = \frac{1}{2} \iint \frac{d\mathbf{r}_1 d\mathbf{r}_2}{r_{12}} \rho(\mathbf{r}_1) \rho(\mathbf{r}_2), \quad (39)$$

$$-K_{XC}[\rho_\alpha, \rho_\beta] = -\frac{1}{2} \iint \frac{d\mathbf{r}_1 d\mathbf{r}_2}{r_{12}} \rho(\mathbf{r}_1, \mathbf{r}_2) \rho(\mathbf{r}_2, \mathbf{r}_1), \quad (40)$$

$$H_{ES}[\Gamma_\alpha, \Gamma_\beta] = -2 \iint \frac{d\mathbf{r}_1 d\mathbf{r}_2}{r_{12}} Q(\mathbf{r}_1, \mathbf{r}_2) Q(\mathbf{r}_2, \mathbf{r}_1) (s_1, s_2), \quad (41)$$

$$Q(\mathbf{r}_1, \mathbf{r}_2) = \rho_\alpha(\mathbf{r}_1, \mathbf{r}_2) - \rho_\beta(\mathbf{r}_1, \mathbf{r}_2), \quad (42)$$

$$\Delta E_{UHFD}^{corr}[\Gamma_\alpha, \Gamma_\beta] = -2 \iint \frac{d\mathbf{r}_1 d\mathbf{r}_2}{r_{12}} [\rho_\alpha(\mathbf{r}_1, \mathbf{r}_2) \rho_\beta(\mathbf{r}_2, \mathbf{r}_1) + \rho_\beta(\mathbf{r}_1, \mathbf{r}_2) \rho_\alpha(\mathbf{r}_2, \mathbf{r}_1)] (s_1, s_2), \quad (43)$$

where $T[\rho]$ represents the expected value of the electron kinetic energy operator T , although this notation does not mean any explicit functional form of ρ , the other explicit energy functionals of ρ have usual meanings, and $H_{ES}[\Gamma_\alpha, \Gamma_\beta]$ does the spin density coupling energy functional between two NMO-fermions, which is expected to contain H_{ex} . (CORREGENDUM: Please add a miss-dropped factor, 2, in Eq. (3.18) in [13], just like above Eq. (41)).

[Proof of Eqs. (36)–(42)] Substituting Eq. (28) into Eq. (29), we get the NMO expansion formula of the exchange-product matrix:

$$\begin{aligned} \Gamma(\mathbf{x}_1, \mathbf{x}'_2) \Gamma(\mathbf{x}_2, \mathbf{x}'_1) &= \sum_{\sigma, m\sigma}^M f_{m\sigma}(\mu_\sigma) \Phi_{m\sigma}(\mathbf{r}_1) \Phi_{m\sigma}(\mathbf{r}'_2)^* \\ &\times \sum_{\sigma', m\sigma'}^M f_{m\sigma'}(\mu_{\sigma'}) \Phi_{m\sigma'}(\mathbf{r}_2) \Phi_{m\sigma'}(\mathbf{r}'_1)^* |\xi_{m\sigma}(s_2) \xi_{m\sigma'}(s_1)\rangle \langle \xi_{m\sigma}(s'_1) \xi_{m\sigma'}(s'_2)|. \end{aligned} \quad (44)$$

Here, to restore the spin-pair wave function to the normal-order form, Dirac's spin operator of Eq. (35) needs to be operated to the two-spin function:

$$\xi_{m\sigma}(s_2) \xi_{m\sigma'}(s_1) = P_{12}^\sigma \xi_{m\sigma}(s_1) \xi_{m\sigma'}(s_2). \quad (45)$$

Then, using Eqs. (32), (33), (35), and (45), we can transform Eq. (44) into two different formulas:

$$\begin{aligned} &\Gamma(\mathbf{x}_1, \mathbf{x}'_2) \Gamma(\mathbf{x}_2, \mathbf{x}'_1) \\ &= \rho(\mathbf{r}_1, \mathbf{r}'_2) \rho(\mathbf{r}_2, \mathbf{r}'_1) \left[\frac{1}{2} (1 + \sigma_{1z} \sigma_{2z}) + \frac{1}{4} (\sigma_{1+} \sigma_{2-} + \sigma_{1-} \sigma_{2+}) \right], \end{aligned} \quad (46)$$

$$\begin{aligned} &= \frac{1}{2} [\rho_\alpha(\mathbf{r}_1, \mathbf{r}'_2) \rho_\alpha(\mathbf{r}_2, \mathbf{r}'_1) + \rho_\beta(\mathbf{r}_1, \mathbf{r}'_2) \rho_\beta(\mathbf{r}_2, \mathbf{r}'_1)] \\ &+ \frac{1}{2} [\rho_\alpha(\mathbf{r}_1, \mathbf{r}'_2) \rho_\beta(\mathbf{r}_2, \mathbf{r}'_1) + \rho_\beta(\mathbf{r}_1, \mathbf{r}'_2) \rho_\alpha(\mathbf{r}_2, \mathbf{r}'_1)] \\ &+ \frac{1}{2} Q(\mathbf{r}_1, \mathbf{r}'_2) Q(\mathbf{r}_2, \mathbf{r}'_1) (\sigma_1, \sigma_2) \\ &+ \frac{1}{2} [\rho_\alpha(\mathbf{r}_1, \mathbf{r}'_2) \rho_\beta(\mathbf{r}_2, \mathbf{r}'_1) + \rho_\alpha(\mathbf{r}_1, \mathbf{r}'_2) \rho_\beta(\mathbf{r}_2, \mathbf{r}'_1)] (\sigma_1, \sigma_2), \end{aligned} \quad (47)$$

with the use of the spin density matrix Q of Eq. (42) and the off-diagonal spinors $\sigma_{j\pm}$ of Eq. (48):

$$\sigma_{j\pm} = \sigma_{jx} \pm i\sigma_{jy}, j = 1, 2. \quad (48)$$

Apparently, there exist two decoupling schemes: (1) In Eq. (46) is decoupled a pair of off-diagonal spinor terms, leading to the UHF approximation, and (2) In Eq. (47) decoupled only the last term, leading to the UHFD approximation. In the UHFD approximation, we obtain the functional formula for the internal energy $U[\Gamma_\alpha, \Gamma_\beta]$ in 3D-spin space decomposed into the principal part $U_{UHFD}^0[\Gamma_\alpha, \Gamma_\beta]$ and the secondary part ΔE_{UHFD}^{corr} in Eq. (36). (QED)

Since all the DFT calculations can be made in the binary-spin Hilbert space, we must take the trace of $H_{ES}[\Gamma_\alpha, \Gamma_\beta]$ in Eq. (37) on the 3D-spin coordinates to obtain its functional of $\rho(\rho_\alpha, \rho_\beta)$, which is equal to a half of the principal exchange-correlation energy functional, that is

$$H_{ES}[\rho_\alpha, \rho_\beta] \equiv \text{Tr}_S(H_{ES}[\Gamma_\alpha, \Gamma_\beta]) = -\frac{1}{2}K_{XC}[\rho_\alpha, \rho_\beta]. \quad (49)$$

Using Eq. (49), we also obtain the principal internal energy functional of ρ :

$$U_{UHFD}^0[\rho_\alpha, \rho_\beta] \equiv \text{Tr}_S(U_{UHFD}^0[\Gamma_\alpha, \Gamma_\beta]) = T[\rho] + V_{ne}[\rho] + J[\rho] - K_{XC}[\rho_\alpha, \rho_\beta], \quad (50)$$

which should be equated to the GC ensemble average of the principal part of the Hamiltonian operator in the second quantization representation in the thermal equilibrium state (see Eq. (15)), that is

$$\hat{H}_{UHFD}^0 = \sum_{\tau}^M \epsilon_{\tau} \hat{a}_{\tau}^{\dagger} \hat{a}_{\tau}, \quad (51)$$

leading to

$$U_{UHFD}^0[\rho_\alpha, \rho_\beta] \equiv \text{Tr}_M[\Gamma \hat{H}_0] = \int d\mathbf{r} \sum_{\tau}^M f_{\tau}(\epsilon_{\tau} - \mu_{\sigma(\tau)}) \Phi_{\tau}^*(\mathbf{r}) \Phi_{\tau}(\mathbf{r}). \quad (52)$$

Similarly, U_{UHFD}^0 can be expanded as the GC ensemble average of a self-consistent effective Hamiltonian as given by

$$U_{UHFD}^0[\rho_\alpha, \rho_\beta] = \int d\mathbf{r} \left\{ \sum_{\tau}^M f_{\tau}(\epsilon_{\tau} - \mu_{\sigma(\tau)}) \Phi_{\tau}^*(\mathbf{r}) \times \left[-\frac{1}{2} \nabla^2 \Phi_{\tau}(\mathbf{r}) + \int v_{NMO}(\mathbf{r}, \mathbf{r}') \Phi_{\tau}(\mathbf{r}') d\mathbf{r}' \right] \right\}, \quad (53)$$

with the use of the local and non-local NMO-based effective potential defined by

$$v_{NMO}(\mathbf{r}, \mathbf{r}') = \left[v(\mathbf{r}, \epsilon) + \frac{1}{2} \int d\mathbf{r}'' \frac{\rho(\mathbf{r}'')}{|\mathbf{r} - \mathbf{r}''|} \right] \delta(\mathbf{r} - \mathbf{r}') - \frac{\rho(\mathbf{r}, \mathbf{r}')}{2|\mathbf{r} - \mathbf{r}'|}, \quad (54)$$

$$\rho(\mathbf{r}) = \sum_{\tau}^M f_{\tau}(\epsilon_{\tau} - \mu_{\sigma(\tau)}) |\Phi_{\tau}(\mathbf{r})|^2, \quad (55)$$

$$\rho(\mathbf{r}, \mathbf{r}') = \sum_{\tau}^M f_{\tau}(\epsilon_{\tau} - \mu_{\sigma(\tau)}) \Phi_{\tau}^*(\mathbf{r}') \Phi_{\tau}(\mathbf{r}). \quad (56)$$

From equivalent Eqs. (52) and (53) leading to Eq. (57), we obtain a series of central Schrödinger equations, (58) by putting $[\dots]_\tau = 0$:

$$U_{UHFD}^0[\rho_\alpha, \rho_\beta] - \text{Tr}_M[\Gamma \hat{H}_0] = \int d\mathbf{r} \left\{ \sum_\tau^M f_\tau(\epsilon_\tau - \mu_{\sigma(\tau)}) \Phi_\tau^*(\mathbf{r}) \right. \quad (57)$$

$$\left. \left[-\frac{1}{2} \nabla^2 \Phi_\tau(\mathbf{r}) + \int v_{NMO}(\mathbf{r}, \mathbf{r}') \Phi_\tau(\mathbf{r}') d\mathbf{r}' - \epsilon_\tau \Phi_\tau(\mathbf{r}) \right] \right\} = 0$$

$$-\frac{1}{2} \nabla^2 \Phi_\tau(\mathbf{r}) + \int d\mathbf{r}' v_{NMO}(\mathbf{r}, \mathbf{r}') \Phi_\tau(\mathbf{r}') = \epsilon_\tau \Phi_\tau(\mathbf{r}), \quad (58)$$

and h.c. for all $\tau \in M$.

This central (not variational!) solution will be stocked as the presumed GC ensemble M , in which the eigenvalues $\{\epsilon_\tau\}$ are usually assumed to be rearranged from the minimum $\epsilon_{1\sigma}$ to the maximum $\epsilon_{M\sigma}$ in the order of increasing energies, first for α -spin NMOs and second for β -spin NMOs, as

$$\tau = 1_\alpha, 2_\alpha, \dots, M_\alpha, 1_\beta, 2_\beta, \dots, M_\beta = 1, 2, \dots, M \quad (M = M_\alpha + M_\beta). \quad (59)$$

For simplicity, we assume that there exists no degeneracy in energy levels in the unrestricted large system without any structural symmetry.

On the other hand, the secondary correlation energy functional, $\Delta E_{UHFD}^{corr}[\Gamma_\alpha, \Gamma_\beta]$, defined by Eq. (43), represents the sole perturbation term in 3D-spin space. Taking the trace of it on the 3D-spin coordinates, we obtain the second quantization expression of it as follows

$$\begin{aligned} \hat{H}_{UHFD}^1 &= \text{Tr}_s(\Delta E_{UHFD}^{corr}[\Gamma_\alpha, \Gamma_\beta]) \\ &= -\frac{1}{2} \iint \frac{d\mathbf{r}_1 d\mathbf{r}_2}{r_{12}} \text{Tr}_s \{ [\rho_\alpha(\mathbf{r}_1, \mathbf{r}_2) \rho_\beta(\mathbf{r}_2, \mathbf{r}_1) + \rho_\beta(\mathbf{r}_1, \mathbf{r}_2) \rho_\alpha(\mathbf{r}_2, \mathbf{r}_1)] (\boldsymbol{\sigma}_1, \boldsymbol{\sigma}_2) \} \\ &= -\sum_{m\alpha}^{\alpha M} \sum_{m\beta}^{\beta M} f(\epsilon_{m\alpha} - \mu_\alpha) f(\epsilon_{m\beta} - \mu_\beta) \iint \frac{d\mathbf{r}_1 d\mathbf{r}_2}{r_{12}} \\ &\quad \times [\Phi_{m\alpha}^*(\mathbf{r}_2) \Phi_{m\alpha}(\mathbf{r}_1) \Phi_{m\beta}^*(\mathbf{r}_1) \Phi_{m\beta}(\mathbf{r}_2)] (\sigma_{+,m\alpha}, \sigma_{-,m\beta} + \sigma_{-,m\alpha} \sigma_{+,m\beta}) \\ &= -\sum_{m\alpha}^{\alpha M} \sum_{m\beta}^{\beta M} (\sigma_{+,m\alpha}, \sigma_{-,m\beta} + \sigma_{-,m\alpha} \sigma_{+,m\beta}) \iint \frac{d\mathbf{r}_1 d\mathbf{r}_2}{r_{12}} \\ &\quad \times [\Phi_{m\alpha}^*(\mathbf{r}_2) \Phi_{m\beta}^*(\mathbf{r}_1) \Phi_{m\beta}(\mathbf{r}_2) \Phi_{m\alpha}(\mathbf{r}_1)] \hat{a}_{m\beta}^\dagger \hat{a}_{m\beta} \hat{a}_{m\sigma}^\dagger \hat{a}_{m\alpha}. \end{aligned} \quad (60)$$

The first-order perturbation term vanishes owing to the nondiagonal spinors. However, the second-order perturbation correction can always induce a finite attractive force between any pair of NMO-fermions with antiparallel spins. The most interesting example would be a positive enhancement effect on the Cooper-pair superconductivity due to an additional attractive force between two conductive Bloch-electrons with antiparallel spins near Fermi level, as will be discussed in Section 2.4.

2.3 MGC-SDFT-UHFD method for polynuclear transition metal complexes

We next consider a variety of paramagnetic systems including plural n (≥ 2) spins, designated $\{\mathbf{S}_i, i = 1, \dots, n\}$, which arise from transition metal (TM) cations, C/N/O-radicals, -C=C- bond radicals, and so on. These spins are quantum-mechanically interacting with each other via the exchange coupling constants ($J_{i,j}$) in the Heisenberg spin Hamiltonian defined by

$$H_{ex} = -2 \sum_{i=1}^{n-1} \sum_{j=i+1}^n J_{ij} (\mathbf{S}_i, \mathbf{S}_j). \quad (61)$$

However, this H_{ex} model takes account only the pure spin operators $\{\mathbf{S}_i\}$ but does not contain any kind of polarized spins of ligand atoms, designated $\{\mathbf{s}_{iL}\}$, "Why?" The most fundamentally important question is, "What is the origin of H_{ex} ?" These questions have been recently solved by Kusunoki [13], as reviewed in this subsection. Let us investigate what kinds of spin-dependent physical processes are involved in the spin-density coupling energy functional $H_{ES}[\Gamma_\alpha, \Gamma_\beta]$ of Eqs. (41) and (42).

Since in the binary spin space appear 2^{n-1} ($n \geq 2$) mutually-independent up/down- i ES arrangements (ESA), which represent one ferromagnetic and the other anti-ferromagnetic states, we must prepare a set of multiple grand canonical (MGC) ensembles, as given by

$$\mathbf{M} = \sum_{k=1}^{2^{n-1}} \mathbf{M}^{(k)}, \mathbf{M}^{(k)} = {}^\alpha \mathbf{M}^{(k)} + {}^\beta \mathbf{M}^{(k)}; \quad (62)$$

$${}^\sigma \mathbf{M}^{(k)} \equiv \left\{ \Psi_{m\sigma}^{(k)}(\mathbf{x}), \epsilon_{m\sigma}^{(k)}, f_{m\sigma}^{(k)} \left(\epsilon_{m\sigma}^{(k)} - \mu_\sigma^{(k)} \right); m\sigma = 1, \dots, M_\sigma \right\}; \sigma = \alpha, \beta. \quad (63)$$

Practically, we can calculate only a set of 2^{n-1} principal internal energy functionals:

$$U_{UHFD}^{(k)}[\rho_\alpha^{(k)}, \rho_\beta^{(k)}] = T^{(k)}[\rho] + V_{ne}^{(k)}[\rho] + J^{(k)}[\rho] - K_{XC}^{(k)}[\rho_\alpha^{(k)}, \rho_\beta^{(k)}]; k = 1, \dots, 2^{n-1}. \quad (64)$$

However, the origin of H_{ex} must be traced to a set of 2^{n-1} equality relationships between the principal exchange-correlation energy functional, $-K_{XC}^{(k)}[\rho_\alpha^{(k)}, \rho_\beta^{(k)}]$, and the projected value of the spin-dependent XC energy functional, i.e.

$$-K_{XC}^{(k)}[\rho_\alpha^{(k)}, \rho_\beta^{(k)}] = 2H_{ES}^{(k)}[\rho_\alpha^{(k)}, \rho_\beta^{(k)}] = 2\text{Tr}_s \left(H_{ES}^{(k)}[\Gamma_\alpha^{(k)}, \Gamma_\beta^{(k)}] \right); k = 1, \dots, 2^{n-1}. \quad (65)$$

We note that the k th projected value of $(\mathbf{S}_i, \mathbf{S}_j)$ onto the binary Hilbert space spanned by the k th GC ensemble $\mathbf{M}^{(k)}$ must depend not only on the k th principal exchange-correlation energy between i ES and j ES, but also on the polarized spins of bridging and non-bridging ligand atoms, $iLaj$ ($j \neq i$) and $iLnb$, respectively, via the conservation law of each projected spin number of $n_i^{(k)}$ and $n_j^{(k)}$, defined by

$$n_i^{(k)} \equiv 2S_i \sigma_{z,i}^{(k)}; \sigma_{z,i}^{(k)} = \pm 1, k = 1, \dots, 2^{n-1}; i = 1, \dots, n. \quad (66)$$

$$\sum_{i=1}^n S_i \sigma_{z,i}^{(k)} \geq 0, k = 1, \dots, 2^{n-1}. \quad (67)$$

Although the arrangement order of n ESA-codes $\left\{ \sigma_{z,i}^{(k)} = 1 \text{ or } -1, i = 1 - n \right\}$ leaves the choice of one's best depending on the arrangement order of n TM-cation spins $\{S_i, -1 - n\}$, a non-negative sum rule of Eq. (67) must be satisfied owing to the time-reversal symmetry.

For the i th transition metal (TM) cations, its non-bridging ligand atoms $iLnb$ and its bridging ligand atoms $iLaj$ between the i th and j th TM-cations, this wave-packet spin projection may be entrusted to the respective spin operator by itself, that is S_i , s_{iLnb} and s_{iLaj} , by imposing each projection equation acting on a spin-dependent AO in a LCAO-NMO wave function, without change of the F-D distribution for the former two and with change to its half distribution for the latter one:

$$S_i g_l^a(\mathbf{x}) = \delta_{a,i} \delta_{l,3d} S_i g_{3d}^i(\mathbf{x}), \quad (68)$$

$$s_{iLnb} g_l^a(\mathbf{x}) = \delta_{a \in iLnb} \delta_{l,2p} s_{iLnb} g_{2p}^{iLnb}(\mathbf{x}), \quad (69)$$

$$s_{iLaj} g_l^a(\mathbf{x}) = \delta_{a \in iLaj} \delta_{l,2p} s_{iLaj} g_{2p}^{iLaj}(\mathbf{x}); f_{iLajm\sigma} = \frac{f_{im\sigma}}{\nu_{iLaj}} = \frac{f_{im\sigma}}{2}, \quad (70)$$

where we have introduced the share frequency $\nu_{iLajm\sigma}$ among n different subsets (in this case, it is 2), $\delta_{a \in A} = (1 \text{ for } a \in A; 0 \text{ for otherwise})$ and $\delta_{x,y}$ is Kronecker's δ .

Concomitantly, the k th GC ensemble $\mathbf{M}^{(k)}$ might be decomposed into n spin-dependent NMO-subsets associated with these elements, and the other spin-free subset as in Eq. (71), each $\mathbf{M}_i^{(k)}$ further decomposed into three components as in Eqs. (72) and (73), finally to define the i th ES in terms of two components in Eq. (74).

$$\mathbf{M}^{(k)} = \sum_{i=1}^n \mathbf{M}_i^{(k)} + \mathbf{M}'^{(k)}, \quad (71)$$

$$\mathbf{M}_i^{(k)} = \mathbf{M}_{id}^{(k)} + \mathbf{M}_{iL}^{(k)} + \mathbf{M}_{io}^{(k)}, \quad (72)$$

$$\mathbf{M}_{iL}^{(k)} = \sum_{j \neq i}^n \mathbf{M}_{iLaj}^{(k)} + \mathbf{M}_{iLnb}^{(k)}, \quad (73)$$

$$\mathbf{M}_{iES}^{(k)} = \mathbf{M}_{id}^{(k)} + \sum_{j \neq i}^n \mathbf{M}_{iLaj}^{(k)}, \quad (74)$$

where the i th subset in Eq. (72) consists of the subset $\mathbf{M}_{id}^{(k)}$ associated with (3d, 4 s, 4p)-electron AO's in the i th TM cation, the subset $\mathbf{M}_{iL}^{(k)}$ associated with 2p-valence electron AO's in the iL th assembly of ligand atoms, and the subset $\mathbf{M}_{io}^{(k)}$ associated with other doubly-occupied core-shell AO's in the i th TM cation. The iL th subset in Eq. (73) can be further decomposed into two kinds of ligand assembly: (1) a *thermal equipartition* half of the $iLaj$ th assembly of bridging ligand atoms between the i th and j th TM cations, which can mediate the antiferromagnetic super-exchange coupling, and (2) the $iLnb$ th assembly of non-bridging ligand atoms around the i th TM cation, which can be either paramagnetically or diamagnetically polarized depending on the ligand C/N/O atomic structure and hence control the i th ES magnitude via the *spin number* (n_i) *conservation law* governing the Mulliken atomic spin densities $\{M_a^{(k)}\}$ [14] of these magnetically-interacting atoms, finally to define the i th ES density $n_{iEF}^{(k)}$ so as to satisfy Eq. (76):

$$n_{iEF}^{(k)} \equiv M_{id}^{(k)} + \sum_{j \neq i}^n \sum_{iLaj} \frac{M_{iLaj}^{(k)} \vartheta \left(M_{iLaj}^{(k)} \sigma_{z,i}^{(k)} \right)}{\nu_{iLaj}^{(k)}} + \delta_{k>1} \sum_{j \neq i}^n \sum_{iLaj} \sigma_{z,i}^{(k)} \frac{M_{iLaj}^{(1)} \vartheta \left(-\sigma_{z,j}^{(1)} \sigma_{z,i}^{(1)} \right)}{\nu_{iLaj}^{(1)}}; \quad (75)$$

$$n_{iLnb}^{(k)} \equiv \sum_{iLnb'} M_{iLnb'}^{(k)}; n_{iEF}^{(k)} + n_{iLnb}^{(k)} = n_i, k = 1(\text{F}), 2(\text{AF}), \dots, 2^{n-1}(\text{AF}). \quad (76)$$

Here, $\vartheta(\text{sign}1 * \text{sign}2)$ is the Heaviside step function, and $\nu_{iLaj}^{(k)}$ is the frequency of the $iLaj$ spin density shared by plural ESs with the same sign, which can be calculated as

$$\nu_{iLaj}^{(k)} = 1 + \vartheta \left(\sigma_{z,i}^{(k)} \sigma_j^{(k)} \right) \text{ for all } k\text{'s}, \quad (77)$$

(CORRIGENDAM: Eq. (5.6c) in [13] should be replaced by Eq. (77)).

Decomposition into these NMO-subsets allows us to provide a noble systematic and quantitative method to derive a set of the expected values of $H_{\text{ex}} \{ \langle H_{\text{ex}} \rangle^{(k)}; k = 1, \dots, 2^{n-1} \}$ from the spin-dependent XC energy functional in Eq. (65), as follows:

The k th spin density matrix for Eq. (42) can be decomposed into

$$Q^{(k)}(\mathbf{r}, \mathbf{r}') = \sum_{\sigma=\alpha}^{\beta} (-1)^{\sigma} \sum_{m\sigma}^{\sigma \mathbf{M}^{(k)}} f_{m\sigma} \Phi_{m\sigma}(\mathbf{r}) \Phi_{m\sigma}(\mathbf{r}')^*; (-1)^{\alpha/\beta} = \pm 1, \quad (78)$$

$$= \sum_{i=1}^n \left[Q_{iES}^{(k)}(\mathbf{r}, \mathbf{r}') + Q_{iLnb}^{(k)}(\mathbf{r}, \mathbf{r}') + Q_{io}^{(k)}(\mathbf{r}, \mathbf{r}') \right] + Q'^{(k)}(\mathbf{r}, \mathbf{r}'), \quad (79)$$

$$= \sum_{i=1}^n \left[Q_{iES}^{(k)}(\mathbf{r}, \mathbf{r}') + Q_{iLnb}^{(k)}(\mathbf{r}, \mathbf{r}') \right] \quad (80)$$

$$+ \sum_{i=1}^n \left[\rho_{io,\alpha}^{(k)}(\mathbf{r}, \mathbf{r}') - \rho_{io,\beta}^{(k)}(\mathbf{r}, \mathbf{r}') \right] + \rho'_{\alpha}{}^{(k)}(\mathbf{r}, \mathbf{r}') - \rho'_{\beta}{}^{(k)}(\mathbf{r}, \mathbf{r}'),$$

in which Eq. (80) indicates that the first term will contribute to both intra-atomic and interatomic spin-density coupling energies generated by open 3d-shell electrons, as given by

$$2H_{ES1}^{(k)} \left[\rho_{\alpha}^{(k)}, \rho_{\beta}^{(k)} \right] \equiv 2E_{ES1}^{(k)} = - \sum_{i=1}^n J_{i,i}^{(k)} S_i (S_i + 1), \quad (81)$$

$$J_{i,i}^{(k)} \equiv \frac{1}{2n_i^2} \iint \frac{d\mathbf{r}_1 d\mathbf{r}_2}{r_{12}} \left[\rho_{iES}^{(k)}(\mathbf{r}_1, \mathbf{r}_2) + \rho_{iLnb}^{(k)}(\mathbf{r}_1, \mathbf{r}_2) \right] \left[\rho_{iES}^{(k)}(\mathbf{r}_2, \mathbf{r}_1) + \sigma_{iLnb}^{(k)}(\mathbf{r}_2, \mathbf{r}_1) \right], \quad (82)$$

and

$$2H_{ES2}^{(k)} \left[\rho_{\alpha}^{(k)}, \rho_{\beta}^{(k)} \right] = 2E_{ES2}^{(k)} = \langle H_{\text{ex}} \rangle^{(k)} = -2 \sum_{i < j}^n J_{i,j} \langle (\mathbf{S}_i, \mathbf{S}_j) \rangle^{(k)}, \quad (83)$$

$$\langle (\mathbf{S}_i, \mathbf{S}_j) \rangle^{(k)} = \text{Tr} \left[(\mathbf{S}_i, \mathbf{S}_j) \Gamma_2^{(k)}(\mathbf{x}_1 \mathbf{x}_2, \mathbf{x}_1 \mathbf{x}_2) \right], \quad (84)$$

$$= \sum_{M_i = -S_i}^{S_i} \sum_{M_j = -S_j}^{S_j} \text{Tr} \left[\langle M_i, M_j | (\mathbf{S}_i, \mathbf{S}_j) | M_i, M_j \rangle \times \langle M_i, M_j | \Gamma_{i,j}^{(k)}(\mathbf{x}_1 \mathbf{x}_2, \mathbf{x}_1 \mathbf{x}_2) | M_i, M_j \rangle \right], \quad (85)$$

with

$$\Gamma_{ij}^{(k)}(\mathbf{x}_1\mathbf{x}_2, \mathbf{x}_1\mathbf{x}_2) = \frac{2}{2} \left[\Gamma_{iES}^{(k)}(\mathbf{x}_1, \mathbf{x}_1)\Gamma_{jES}^{(k)}(\mathbf{x}_2, \mathbf{x}_2) - \Gamma_{iES}^{(k)}(\mathbf{x}_1, \mathbf{x}_2)\Gamma_{jES}^{(k)}(\mathbf{x}_2, \mathbf{x}_1) \right], \quad (86)$$

respectively, and the second and third terms to a major H_{ex} -less component in the principal XC energy, as given by

$$-K_{XC-H_{ex}}^{(k)}[\rho_\alpha^{(k)}, \rho_\beta^{(k)}] = 2H_{ES0}^{(k)}[\rho_{ES0,\alpha}^{(k)}, \rho_{ES0,\beta}^{(k)}] = 2E_{ES0}^{(k)}, \quad (87)$$

$$= -\frac{1}{2} \iint \frac{d\mathbf{r}_1 d\mathbf{r}_2}{r_{12}} \left[\rho^{(k)}(\mathbf{r}_1, \mathbf{r}_2) - \sum_{i=1}^n \left\{ \rho_{iES}^{(k)}(\mathbf{r}_1, \mathbf{r}_2) + \rho_{iLnb}^{(k)}(\mathbf{r}_1, \mathbf{r}_2) \right\} \right] \times \left[\rho^{(k)}(\mathbf{r}_2, \mathbf{r}_1) - \sum_{i=1}^n \left\{ \rho_{iES}^{(k)}(\mathbf{r}_2, \mathbf{r}_1) + \rho_{iLnb}^{(k)}(\mathbf{r}_2, \mathbf{r}_1) \right\} \right]; \quad (88)$$

To calculate Eq. (84), we need the total spin operator given by

$$\mathbf{S}_{tot} = \sum_{i=1}^n \left(\mathbf{S}_i + \sum_{iLaj} \mathbf{s}_{iLaj} + \sum_{iLnb} \mathbf{s}_{iLnb} \right), \quad (89)$$

The i th ES spin operator, \mathbf{S}_i , is considered to turn around between up and down states, $|S_i\rangle$ and $|-S_i\rangle$, in the binary Hilbert space spanned by two rules:

$$\sum_{M_i=-S_i}^{S_i} |M_i\rangle\langle M_i| = \mathbf{1}_i; i = 1, \dots, n, \quad (90)$$

and

$$\langle \alpha_i | M_i \rangle = \frac{\delta_{M_i, S_i}}{\sqrt{|n_i|}}, \langle \beta_i | M_i \rangle = \frac{\delta_{M_i, -S_i}}{\sqrt{|n_i|}}; \quad (91)$$

while the $iLaj$ th and $iLnb$ th ES spin operators, \mathbf{s}_{iLaj} and \mathbf{s}_{iLnb} , are assumed to automatically respond to the up or down state of \mathbf{S}_i . Then, the expected value of the z-component of \mathbf{S}_{tot} in the k th ESA state is given by

$$\langle S_{tot,z} \rangle^{(k)} = \sum_{i=1}^n \text{Tr} \left\{ \mathbf{S}_{i,z} \left[\Gamma_{iES}^{(k)}(\mathbf{x}, \mathbf{x}) + \Gamma_{iLnb}^{(k)}(\mathbf{x}, \mathbf{x}) \right] \right\}, \quad (92)$$

$$= \sum_{i=1}^n S_i \sigma_{z,i}^{(k)} \left(P_{iES}^{(k)} + P_{iLnb}^{(k)} \right) = \sum_{i=1}^n S_i \sigma_{z,i}^{(k)}, \quad (93)$$

$$\Gamma_{iES}^{(k)}(\mathbf{x}, \mathbf{x}') = \Gamma_{id}^{(k)}(\mathbf{x}, \mathbf{x}') + \sum_{j \neq i} \sum_{iLaj'} \Gamma_{iLaj'}^{(k)}(\mathbf{x}, \mathbf{x}'), \quad (94)$$

$$P_{iES}^{(k)} = \frac{n_{iES}^{(k)}}{n_i} = \frac{1}{n_i} \int d\mathbf{r} Q_{iES}^{(k)}(\mathbf{r}, \mathbf{r}), \quad (95)$$

$$P_{iLnb}^{(k)} = \frac{n_{iLnb}^{(k)}}{n_i} = \frac{1}{n_i} \int d\mathbf{r} Q_{iLnb}^{(k)}(\mathbf{r}, \mathbf{r}), \quad (96)$$

$$P_{iES}^{(k)} + P_{iLnb}^{(k)} = \left[n_{iES}^{(k)} + n_{iLnb}^{(k)} \right] / n_i = 1. \quad (97)$$

It is important to remind that the last additional term in Eq. (75) in the antiferromagnet kAF th ESA state was absolutely required for a systematic better agreement with experimental $J_{i,j}$ indicating that a large-positive $M_{iLaj}^{(1F)}$ density in the $1F$ th-ESA state can be divided into two half densities which will be reversed to be distributed with phase matching to an antiferromagnetic pair of $n_{iES}^{(kAF)}$ and $n_{jES}^{(kAF)}$ in the kAF th ESA state, as given by a programmatic equation [13],

$$M_{iLaj}^{(k)} \Leftarrow \frac{1}{2} \sigma_{z,i}^{(k)} M_{iLaj}^{(1)} \vartheta \left(-\sigma_{z,i}^{(k)} \sigma_{z,j}^{(k)} \right) + M_{iLaj}^{(k)}. \quad (98)$$

Now, substituting Eq. (86) into Eq. (85) and taking the traces over spin-orbital coordinates with use of Eqs. (90), (91), (95) and (96), we obtain a noble formula

$$\langle (\mathbf{S}_i, \mathbf{S}_j) \rangle^{(k)} = n_{iES}^{(k)} n_{jES}^{(k)} \left(1 - S_{iES,jES}^{(k)} \right), \quad (99)$$

$$S_{iES,jES}^{(k)} \equiv \frac{\text{Tr} \left[\Gamma_{iES}^{(k)}(\mathbf{x}_1, \mathbf{x}_2) \Gamma_{jES}^{(k)}(\mathbf{x}_2, \mathbf{x}_1) \right]}{\text{Tr} \left[\Gamma_{iES}^{(k)}(\mathbf{x}_1, \mathbf{x}_1) \right] \text{Tr} \left[\Gamma_{jES}^{(k)}(\mathbf{x}_1, \mathbf{x}_1) \right]}, k = 1, \dots, 2^{n-1}. \quad (100)$$

Here, $\{S_{iES,jES}^{(k)}\}$ represents a set of the Exchange-Correlation vs. Classical Coulomb Density Overlap Integral (XC/CC-DOI) ratios. Although it appears almost impossible to directly calculate a set of $2^{n-2}n(n-1)$ XC/CC-DOI ratios, we could find out a reasonable solution of Eq. (103) by imposing 2^{n-1} equations to eliminate all the residues $\{\Delta^2 \langle \mathbf{S}_{tot}^2 \rangle^{(k)}\}$ from a set of the expected values of $\{\langle \mathbf{S}_{tot}^2 \rangle^{(k)}\}$, which are given by

$$\langle \mathbf{S}_{tot}^2 \rangle^{(k)} = \langle \mathbf{S}_{tot,z} \rangle^{(k)} \left[\langle \mathbf{S}_{tot,z} \rangle^{(k)} + 1 \right] + \sum_{i=1}^n S_i \left(1 - \sigma_{z,i}^{(k)} \right) + \Delta^2 \langle \mathbf{S}_{tot}^2 \rangle^{(k)}, \quad (101)$$

$$\Delta^2 \langle \mathbf{S}_{tot}^2 \rangle^{(k)} = \sum_{i=1}^n S_i^2 \left[1 - \left(P_{iES}^{(k)} \right)^2 \right] - \frac{1}{2} \sum_{i < j} n_{iES}^{(k)} n_{jES}^{(k)} S_{iES,jES}^{(k)} = 0, \quad (102)$$

$$S_{iES,jES}^{(k)} = \frac{4}{n(n-1)} \left\{ \sum_{i'=1}^n S_{i'}^2 \left[1 - \left(n_{i'ES}^{(k)} / 2S_{i'}^{(k)} \right)^2 \right] \right\} \left(n_{iES}^{(k)} n_{jES}^{(k)} \right)^{-1}; k = 1, \dots, 2^{n-1}, \quad (103)$$

Thus, we could derive the MGC-set of the internal energy functionals taking each different decomposition form from Eq. (64) involving the projected Heisenberg spin Hamiltonian:

$$\langle H_{ex} \rangle^{(k)} = -\frac{1}{2} \sum_{i < j}^n J_{i,j} \left(1 - S_{iES,jES}^{(k)} \right) n_{iES}^{(k)} n_{jES}^{(k)}, k = 1, \dots, 2^{n-1}, \quad (104)$$

$$U_{UHFD-H_{ex}}^{(k)}[\rho] = T^{(k)}[\rho] + V_{en}^{(k)}[\rho] + J^{(k)}[\rho] - K_{XC-Hex}^{(k)} \left[\rho - \sum_{i=1}^n \{ \rho_{iES} + \rho_{iLnb} \} \right], \quad (105)$$

$$U_{UHFD}^{(k)}[\rho_\alpha, \rho_\beta] = U_{UHFD-H_{ex}}^{(k)}[\rho] + \langle H_{ex} \rangle^{(k)}. \quad (106)$$

Notably, one may expect that the H_{ex} -less internal energy function defined by Eq. (106) will become almost constant over 2^{n-1} ESA states, owing to the sum of four different components with each having a weak k -dependency. If this is the case, one can utilize Eqs. (104) and (106) to determine the only unknown set of mean ES-exchange coupling constants, $\{J_{i,j}; i(j > i) = 1, \dots, n\}$, since $n2^{n-1}$ effective spin densities $\{n_{iES}^{(k)}\}$, $2^{n-2}n(n-1)$ XC/CC-DOI ratios defined by Eq. (103) and $(2^{n-1}-1)$ energy-difference equations (107) could be quantitatively calculated using UB3LYP/PBS(ϵ_6)/lacvp** method:

$$\Delta U_{UHFD}^{(k)}[\rho_\alpha, \rho_\beta] \equiv U_{UHFD}^{(k)}[\rho_\alpha, \rho_\beta] - U_{UHFD}^{(1)}[\rho_\alpha, \rho_\beta] \cong \langle H_{ex} \rangle^{(k)} - \langle H_{ex} \rangle^{(1)}; k = 2, \dots, 2n - 1, \quad (107)$$

so that the transformed equations can be written in regular matrix form:

$$A^T A X = A^T B, \quad (108)$$

$$A = -\frac{1}{2} \begin{bmatrix} \Delta \left[\left(1 - S_{1ES,2ES}^{(2)} \right) n_{1ES}^{(2)} n_{2ES}^{(2)} \right] & \cdots & \Delta \left[\left(1 - S_{(n-1)ES,nES}^{(2)} \right) n_{(n-1)ES}^{(2)} n_{nES}^{(2)} \right] \\ \vdots & \ddots & \vdots \\ \Delta \left[\left(1 - S_{(n-1)ES,nES}^{(2^{n-1})} \right) n_{(n-1)ES}^{(2^{n-1})} n_{nES}^{(2^{n-1})} \right] & \cdots & \Delta \left[\left(1 - S_{(n-1)ES,nES}^{(2^{n-1})} \right) n_{(n-1)ES}^{(2^{n-1})} n_{nES}^{(2^{n-1})} \right] \end{bmatrix}, \quad (109)$$

$$B = (B_2, \dots, B_{2^{n-1}}), B_k = \Delta U_{UHFD}^{(k)} - \Delta U_{UHFD-H_{ex}}^{(k)}; k = 2, \dots, 2^{n-1}, \quad (110)$$

$$X = (X_1, \dots, X_{n(n-1)/2}) \equiv (X_{ij}); X_{ij} = J_{i,j}, \quad (111)$$

where A^T is the transpose of A . Thus, we get a unique solution:

$$J_{i,j} = \left[(A^T A)^{-1} A^T B \right]_{ij}. \quad (112)$$

For $n = 2$, Eq. (112) reduces to

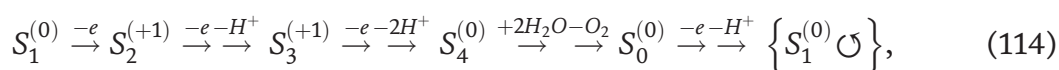
$$J_{1,2} \cong \frac{2\Delta U_{UHFD}^{(2)}}{\left(1 - S_{1ES,2ES}^{(1)} \right) n_{1ES}^{(1)} n_{2ES}^{(1)} - \left(1 - S_{1ES,2ES}^{(2)} \right) n_{1ES}^{(2)} n_{2ES}^{(2)}}. \quad (113)$$

In **Table 1**, we show again the results of benchmark-test calculations of the ES-exchange coupling constants $J_{1,2}$, designated $(J_{1,2/a}^{(m)}, J_{1,2/c}^{(m)}, \dots, J_{1,2/k}^{(m)})$, for 10 biomimetic binuclear Cu, Mn and Fe complexes, named (**a**, **c**, ..., **k**), were made using 13 conventional m XC/PBS/lacvp** method ($m = 4 \sim 16$) in place of the present MGC-SDFT-UHFD ($\equiv 0$ XC) method, which is unfortunately not yet implemented. These data sets were compared with the observed values, named $(J_{1,2/a}^{exp}, J_{1,2/c}^{exp}, \dots, J_{1,2/k}^{exp})$, to show all the excellent quantitative agreements between the theoretical values $(J_{1,2/a}^{(4)}, J_{1,2/c}^{(4)}, \dots, J_{1,2/k}^{(4)})$ and the experimental values mentioned above only by the standard B3LYP ($\equiv 4$ XC) method [13]. Here, we raise two possible explanations for the best performance by the B3LYP hybrid XC energy functional; (1) the best atomic

structure of each TM-dimeric complex could be obtained by further geometry-optimization near the observed XRD structure by the B3LYP/PBS(ϵ)/lacvp** method [15, 16] with the dielectric constant ϵ of the solvent being chosen the best one from 5, 10, 20, and 40 [13]; (2) as *an ideally-good balance between the exchange and correlation energy* in the UHFD approximation is considered to be a key factor, B3LYP/PBS(ϵ)/lacvp** method may satisfy this condition most closely.

2.4 Two most stable isomers of the $S_1^{(0)}$ state Mn_4CaO_5 clusters: Identified by two EPR signals

We have recently applied the UB3LYP/PBS(ϵ)/lacvp** method in place of the UHFD/ PBS(ϵ)/lacvp** method to all the water-splitting and oxygen-evolving reactions catalyzed by the Mn_4CaO_5 cluster in photosystem II (PSII). The electron-abstracting and proton-releasing reactions from the so-called oxygen-evolving complex (OEC) are considered to occur serially via five redox states, called Kok's S_i -states ($i = 0, 1, \dots, 4$), where S_1 is the dark-stable state, and S_4 spontaneously decays to the initial S_0 -state after releasing two protons and evolving dioxygen: the generalized reaction schemes are symbolically given by



where the figure k in the superfix parentheses of $S_i^{(k)}$ represents a formal charge of the i th OEC, $-e$ above an arrow (\rightarrow) indicate one electron transfer from OEC to $P680^{(+)}$, an oxidized PSII reaction center intermittingly generated by every $\sim 10 \mu s$ light-pulse, $-H^+$ above an arrow (\rightarrow) does a proton released into aqueous phase, and the symbols $+(-)$ indicate to go out(in) of OEC, respectively. Among many controversial problems remained to be elucidated, we here take up the molecular structure of the $S_1^{(0)}$ -state Mn_4CaO_5 cluster, that is not yet established because the experimental data from XFEL, EPR and EXAFS spectroscopies appear to be apparently inconsistent if these are assumed to have been observed from the same $S_1^{(0)}$ -state. Although we can't exclude the possibility that the XFEL model [21] may reflect a photo-reduced $S_0^{(-1)}$ state of the $S_1^{(0)}$ -state Mn_4CaO_5 cluster, we have no reason to doubt the fact that two kinds of broad g4.8 and g12-multiline EPR signals were observed from the $S_1^{(0)}$ -state samples of cyanobacteria [18, 19] and spinach [20], respectively, which must have slightly different structures due to the different peripheral proteins between them. Indeed, we could prove that these EPR signals are attributable to two different structural isomers, named S_{1A} and S_{1B} in [23], which coexist with quasi-degenerate lowest energies in the respective $S_1^{(0)}$ -state. Two papers substantiating these ideas will be submitted for publication near future.

2.5 Superconductivity enhanced by the secondary correlation interaction in metals

It is well known that many materials become superconducting (S-phase) at lower temperatures than the critical temperature T_c where each system makes the transition from the normal metallic phase (N-phase). This phenomenon has been explained in terms of the Bardeen-Cooper-Schrieffer model [23, 24] combining the Fröhlich electron-lattice attractive interaction model [25] and the Bogoliubov Cooper-pairing

model [26]. The highest T_c that had been achieved on 2015 is the sulfur hydride system at 203 K at high pressure (155 GP), identified from the observed magnetization vs. θ/k_B stepping-curve [26]. The observed H/D isotope effect on the down-shift & down-size of this curve appears to be consistent with the BCS model. Drozdov et al. raised three conditions required for such much higher- T_c than those of normal metals: (1) higher-frequency-phonon, (2) stronger electron-phonon coupling, and (3) a higher-density of Cooper pairing states [27]. At least the former two conditions could in principle be fulfilled for metallic and covalent compounds dominated by hydrogen. But notably the BCS model contains a serious deficiency that it is based on the free electron model but not on the Bloch-electron model depending on any approximation of self-consistent exchange-correlation potential, so that it is forced to take account only the screened Coulomb repulsive force between conductive electrons, as given by a Fourier transform,

$$\lim_{\kappa \rightarrow 0^+} \frac{e^2}{r} e^{-\kappa r} = \int V_{sc}(\mathbf{q}) e^{i\mathbf{q} \cdot \mathbf{r}} d\mathbf{q}; V_{sc}(\mathbf{q}) = \lim_{\kappa \rightarrow 0^+} \frac{4\pi e^2}{q^2 + \kappa^2}, \quad (115)$$

where κ is called ‘‘Thomas-Fermi wave number’’ and the limit of $\kappa \rightarrow 0^+$ implies a bare-Coulomb interaction. In order to treat such a many-body effect for Bloch-electrons near the Femi-level μ_F , we should adopt the grand potential Ω as the more appropriate thermodynamic free energy than the internal energy U , as given by

$$\Omega = -pV = U - \mu_F \bar{N} - \theta \Sigma. \quad (116)$$

Although here we assume that the decrease of entropy Σ upon the N-to-S phase transition may be relatively much smaller than the decrease of $U - \mu_F \bar{N}$ at least at low temperatures. This choice of Ω is also consistent with the fact that the higher pressure appears to be directly correlated with higher- T_c superconductors [27].

In contrast to the conventional idea of repulsive Coulomb force, the principal exchange-correlation energy Hamiltonian \hat{H}_{UHFD}^0 of Eq. (57) is already incorporated in the present GC-UHFD-SDFT theory to define a binary set of Bloch eigenstates occupied with the Fermi-Dirac distribution $f(\epsilon_k - \mu_F)$, designated ${}_{\sigma}^{\sigma} \mathbf{M}(\sigma = \alpha, \beta)$, and there remains only the secondary correlation energy part of Eq. (60) to be regarded as giving rise to the attractive exchange force between opposite-spin itinerant Bloch-electrons. Hence, neglecting the entropic term, we need only to treat a small part of the grand potential of Eqs. (116) alone, that can be expanded by the perturbation theory:

$${}_B \Omega_{UHFD} = {}_B \Omega_{UHFD}^0 + {}_B \Omega_{UHFD}^1 + {}_B \Omega_{UHFD}^2 + \dots, \quad (117)$$

$${}_B \hat{\Omega}_{UHFD}^0 \cong {}_B \hat{H}_{UHFD}^0 - \mu_F \sum_{k\sigma} a_{k\sigma}^\dagger a_{k\sigma} = \sum_{\sigma=\alpha,\beta} \sum_{k\sigma} a_{k\sigma}^\dagger [\epsilon_{k\sigma} - \mu_F] a_{k\sigma}, \quad (118)$$

$${}_B \hat{\Omega}_{UHFD}^1 = \sum_{\sigma=\alpha,\beta} \sum_{k\sigma, k'\bar{\sigma}} V_{UHFD}^{k\sigma, k'\bar{\sigma}} V_{k\sigma, k'\bar{\sigma}} a_{k\sigma}^\dagger a_{k'\bar{\sigma}}^\dagger a_{k'\bar{\sigma}} a_{k\sigma}, \quad (119)$$

$$V_{UHFD}^{k\sigma, k'\bar{\sigma}} \equiv -e^2 \iint \frac{d\mathbf{r}_1 d\mathbf{r}_2}{2r_{12}} \Phi_{k\sigma}^*(\mathbf{r}_2) \Phi_{k'\bar{\sigma}}^*(\mathbf{r}_1) \Phi_{k'\bar{\sigma}}(\mathbf{r}_2) \Phi_{k\sigma}(\mathbf{r}_1), \quad (120)$$

$$\times (\sigma_{+,k\sigma} \sigma_{-,k'\bar{\sigma}} + \sigma_{-,k\sigma} \sigma_{+,k'\bar{\sigma}})$$

$$\approx - \lim_{\kappa \rightarrow 0^+} \frac{4\pi e^2 V}{|\mathbf{k} - \mathbf{k}'|^2 + \kappa^2} (\sigma_{+,k\sigma} \sigma_{-,k'\bar{\sigma}} + \sigma_{-,k\sigma} \sigma_{+,k'\bar{\sigma}}), \quad (121)$$

where we put $\bar{\alpha} = \beta$ and $\bar{\beta} = \alpha$, and used the plane-wave approximation for the conductive Bloch-wave functions: $\Phi_{k\sigma}(\mathbf{r}_2) \approx \exp[i\mathbf{k} \cdot \mathbf{r}_2]$, $\Phi_{k\sigma}^*(\mathbf{r}_2) \approx \exp[-i\mathbf{k} \cdot \mathbf{r}_2]$ et c. to make the double integrations on the coordinate vectors \mathbf{r}_1 and \mathbf{r}_2 after transformed into $\mathbf{R}_{12} = (\mathbf{r}_1 + \mathbf{r}_2)/2$ and $\mathbf{r}_{12} = \mathbf{r}_2 - \mathbf{r}_1$, together with introducing the screened-Coulomb damping factor $\exp(-\kappa r_{12})$. Note that the volume of the system V appears from the integral on the center-of-mass coordinate \mathbf{R}_{12} .

Notably, this spin-dependent first-order perturbation of Eq. (120) is off-diagonal in the binary Hilbert space, so that it can't contribute to the renormalized eigenstates (S-state) through any odd-number order of perturbation term. Then, the predominant contribution could arise from the second order perturbation term as given by

$${}_B\Omega_{UHFD}^2 = \sum_{\sigma=\alpha,\beta} \sum_{\mathbf{k}_{1\sigma}}^{\sigma\mathbf{M}} \sum_{\mathbf{k}'_{1\bar{\sigma}}}^{\bar{\sigma}\mathbf{M}} \sum_{\mathbf{k}_{2\sigma}}^{\sigma\mathbf{M}} \sum_{\mathbf{k}'_{2\bar{\sigma}}}^{\bar{\sigma}\mathbf{M}} \frac{V_{UHFD}^{k_1,k'_1} [V_{UHFD}^{k_2,k'_2}]^*}{\epsilon_{k_{1\sigma}} + \epsilon_{k'_{1\bar{\sigma}}} - \epsilon_{k_{2\sigma}} - \epsilon_{k'_{2\bar{\sigma}}}} \quad (122)$$

$$\times f(\epsilon_{k_{1\sigma}} - \mu) f(\epsilon_{k'_{1\bar{\sigma}}} - \mu) [1 - f(\epsilon_{k_{2\sigma}} - \mu)] [1 - f(\epsilon_{k'_{2\bar{\sigma}}} - \mu)],$$

$$V_{UHFD}^{k,k'} = - \lim_{\kappa \rightarrow 0^+} \frac{4\pi e^2 V}{|\mathbf{k} - \mathbf{k}'|^2 + \kappa^2}. \quad (123)$$

Significantly in the second-quantization representation this term may be transformed into

$${}_B\widehat{\Omega}_{UHFD}^2 = \sum_{\sigma=\alpha,\beta} \sum_{\mathbf{k}_{1\sigma}}^{\sigma\mathbf{M}} \sum_{\mathbf{k}'_{1\bar{\sigma}}}^{\bar{\sigma}\mathbf{M}} \sum_{\mathbf{k}_{2\sigma}}^{\sigma\mathbf{M}} \sum_{\mathbf{k}'_{2\bar{\sigma}}}^{\bar{\sigma}\mathbf{M}} V_{UHFD}^{k_1,k'_1;k_2,k'_2} \quad (124)$$

$$\times \widehat{a}_{\mathbf{k}'_{2\bar{\sigma}}} \widehat{a}_{\mathbf{k}'_{2\bar{\sigma}}}^\dagger \widehat{a}_{\mathbf{k}_{2\sigma}} \widehat{a}_{\mathbf{k}_{2\sigma}}^\dagger \widehat{a}_{\mathbf{k}'_{1\bar{\sigma}}} \widehat{a}_{\mathbf{k}'_{1\bar{\sigma}}}^\dagger \widehat{a}_{\mathbf{k}_{1\sigma}} \widehat{a}_{\mathbf{k}_{1\sigma}}^\dagger,$$

$$V_{UHFD}^{k_1,k'_1;k_2,k'_2} = \lim_{\kappa \rightarrow 0^+} \frac{(4\pi e^2 V)^2}{\left(|\mathbf{k}_1 - \mathbf{k}'_1|^2 + \kappa^2\right) \left(|\mathbf{k}_2 - \mathbf{k}'_2|^2 + \kappa^2\right) (\epsilon_{k_1} + \epsilon_{k'_1} - \epsilon_{k_2} - \epsilon_{k'_2})} < 0. \quad (125)$$

The first point to notice is that the second-order perturbation Eq. (122) might be too complicated but could generate the attractive interaction between two Cooper-pair particles if it be approximated by the appropriate form (simply putting $\mathbf{k}'_{i\beta} = -\mathbf{k}_{i\beta}$; $i = 1, 2$ and multiplying twice the state number in each spherical-shell volume, $4\pi k_F^3 \omega_D / \mu_F$, as given by $N(k_F) \approx 4\pi k_F^3 \omega_D / \mu_F (2\pi)^3 V = k_F^3 \omega_D / 2\pi^2 V \mu_F$):

$${}_B\widehat{\Omega}_{UHFD}^2 \approx \sum_{\sigma=\alpha,\beta} \sum_{\mathbf{k}_{1\sigma}}^{\sigma\mathbf{M}} \sum_{\mathbf{k}_{2\sigma}}^{\sigma\mathbf{M}} V_{UHFD}^{k_1,-k_1;k_2,-k_2} \widehat{a}_{-\mathbf{k}_{2\bar{\sigma}}} \widehat{a}_{-\mathbf{k}_{2\bar{\sigma}}}^\dagger \widehat{a}_{\mathbf{k}_{2\sigma}} \widehat{a}_{\mathbf{k}_{2\sigma}}^\dagger \widehat{a}_{-\mathbf{k}_{1\bar{\sigma}}} \widehat{a}_{-\mathbf{k}_{1\bar{\sigma}}}^\dagger \widehat{a}_{\mathbf{k}_{1\sigma}} \widehat{a}_{\mathbf{k}_{1\sigma}}^\dagger, \quad (126)$$

$$V_{UHFD}^{k_1,-k_1;k_2,-k_2} \approx \lim_{\kappa \rightarrow 0^+} \frac{(4\pi e^2)^2 (k_F^3 \omega_D / 2\pi^2 \mu_F)^2}{2(4k_1^2 + \kappa^2)(4k_2^2 + \kappa^2)(\epsilon_{k_1} - \epsilon_{k_2})} < 0; \quad (127)$$

which is an attractive potential under the BCS restrictions:

$$-\omega_D < \epsilon_{k_1} - \mu_F < 0 < \epsilon_{k_2} - \mu_F < \omega_D, \quad (128)$$

where ω_D is the Debye frequency, and note that the matrix element Eq. (126) does not contain V and it is proportional to $\omega_D^2/(\epsilon_{k_2} - \epsilon_{k_1})$, which diverges as $(\epsilon_{k_2} - \epsilon_{k_1}) \rightarrow 0$ and hence may not be approximated as a constant. Examination of this singularity problem must be postponed in future, because of the page limitation.

Up to the present stage, however, we find out that in the principal GC-SDFT-UHFD method the remained secondary correlation interaction between Bloch-electrons near the Fermi-surface could generate an additional attractive force to promote the Cooper-pairing superconductivity by increasing not only the concentration of Cooper-pair particles but also the energy gap at the Fermi level.

3. Conclusion

In this chapter, we have reviewed the MGC-SDFT-UHFD method proposed in [13] in order to advance beyond the conventional KS-DFT-UHF method. We need more clearly to explain why the KS-formalism must be regarded as incomplete, because it is a kind of double standard or hybrid theory based the quantum-mechanical rule in closed system and the thermodynamic rule in open system, as clearly seen from their use of two distinct variation-principal equations. This inconsistent theory results in two problematic notions, (1) “eternally-unknown correlation energy functional” including a separated part of kinetic energy, and (2) a set of mutually interacting LCAO-MO quasi-particles.

Here, we have widely proposed a thermodynamic alternative to derive the principal internal energy functional, which has been required to define the self-consistent one-body potential in the Schrödinger equation yielding the ultimate ground and excited states, further which have been required multiple grand canonical ensembles to properly describe all kinds of spin-dependent systems, like the paramagnetic properties of the water-splitting Mn_4CaO_5 -cluster in photosystem II. This one-body quasi-particle world picture has been completed by our two revolutionary discoveries of the *principal exchange-correlation energy functional*, that is, a non-local exchange-correlation interaction, and a complete set of self-consistent *LCAO-NMOs*, which extensively span all the energy levels below dissociation limit (called the work function W) with the Fermi-Dirac distribution.

Significantly, we have presented in Sections 2.3 and 2.4 two experimental evidences directly supporting the quantitative and systematic aspects of the MGC-SDFT-UHFD method, and in Section 2.5 one more evidence indirectly supporting this UHFD decoupling scheme retaining the only *secondary correlation energy functional*, which spin-dependent interaction between Bloch-electrons can promote Cooper-pairings of Bloch-electrons near Fermi-level in superconductor, provided that their eigen states might be exactly determined by the MGC-SDFT-UHFD method under the crystalline periodic conditions. This implies that the Bloch-electrons near the Fermi surface are unstable in the normal phase and hence tend to make the phase transition to the superconducting phase. Further, this provides an additional mechanism for the high-temperature superconductivity. It is further emphasized that the MGC-SDFT-UHFD/PSB(ϵ)/lacvp** method can help meet the demand for an eagerly awaited, first principle, quantitative, and practical method to elucidate the enzymatic function of paramagnetic Mn_4CaO_x clusters in a series of water-splitting and oxygen-evolving reactions in PSII. Moreover, the present

method have very high potential to be able to extend the application fields to the optical excited states, the van-der Waals interactions between fragments in the molecular system and the high-temperature superconductor.

Acknowledgements


The authors would like to acknowledge the infra-structure support for the Joint Research Programs in Graduate School of Science and Technology, Meiji University, Japan.

Author details

Masami Kusunoki
Meiji University, Kawasaki, Japan

*Address all correspondence to: kusunoki@meiji.ac.jp

IntechOpen

© 2023 The Author(s). Licensee IntechOpen. This chapter is distributed under the terms of the Creative Commons Attribution License (<http://creativecommons.org/licenses/by/3.0>), which permits unrestricted use, distribution, and reproduction in any medium, provided the original work is properly cited. 

References

- [1] Hohenberg P, Kohn W. Inhomogeneous electron gas. *Physical Review*. 1964;**136**(B):864-871. DOI: 10.1103/PhysRev.136.B864
- [2] Kohn W, Sham LJ. Self-consistent equations including exchange and correlation effects. *Physical Review*. 1965;**140**(A):1133-1137. DOI: 10.1103/PhysRev.140.A1133
- [3] Sham LJ. Exchange and correlation in density-functional theory. *Physical Review B*. 1985;**32**:3876-3882. DOI: 10.1103/PhysRevB.32.3876
- [4] Parr RG, Yang W. Density-functional theory of atoms and molecules. In: Breslow R, Goodenough JB, Halpern J, Rowlinson JS, editors. *International Series of Monographs on Chemistry*. New York: Oxford Science; 1989. vol. 16, pp. 1-333. ISBN: 0-19-509276-7
- [5] Dreizler RM, Gross EKV. *Density Functional Theory: An Approach to the Quantum Many-Body Problem*. Berlin: Springer; 1990. pp. 1-302. DOI: 10.1007/978-3-642-86105-5
- [6] Kock W, Holthausen MC. *A Chemist's Guide to Density Functional Theory*. Weinheim: WILEY-VCH; 2000. pp. 1-294. ISBN: 3-527-29918-1
- [7] Becke AD. Perspective: Fifty years of density-functional theory in chemical physics. *Journal of Chemical Physics*. 2014;**140**(18):18A301. DOI: 10.1063/1.4869598
- [8] Sundararaman R, Goddard WA, Alias TA. Grand canonical electronic density functional theory: Algorithms and applications to electrochemistry. *Journal of Chemical Physics*. 2017; **146**:114104-114114. DOI: 10.1063/1.4978411
- [9] Evangelista FA. Perspective: Multireference coupled cluster theories of dynamical electron correlation. *Journal of Chemical Physics*. 2018;**149**:030901-030914. DOI: 10.1063/1.5039496
- [10] Mardirossian N, Head-Gordon M. Thirty years of density functional theory in computational chemistry: An overview and extensive assessment of 200 density functionals. *Molecular Physics*. 2017;**115**:2315-2372. DOI: 10.1080/00268976.2017.1333644
- [11] Kitakawa CK, Maruyama T, Oonari J, Mitsuta Y, Kawakami T, Okumura M, et al. Linear response functions of densities and spin densities for systematic Modeling of the QM/MM approach for mono- and poly-nuclear transition metal systems. *Molecules*. 2019;**24**:821-849. DOI: 10.3390/molecules24040821
- [12] Zhou C, Hermes MR, Wu D, Bao JJ, Pandharkar R, King DS, et al. Electronic structure of strongly correlated systems: Recent developments in multiconfiguration pair density functional theory and multiconfiguration nonclassical-energy functional theory. *Chemical Science*. 2022;**13**:685-7706. DOI: 10.1039/d2sc01022d
- [13] Kusunoki M. Heisenberg spin Hamiltonian derived from a multiple grand canonical spin density functional theory with a principal nonlocal exchange-correlation energy functional. *Journal of Physical Society of Japan*. 2022;**91**:014702-(1-28). DOI: 10.7566/JPSJ.91.014702
- [14] Mulliken RS. Electronic population analysis on LCAO-MO molecular wave functions. I. *Journal of Chemical Physics*. 1955;**23**:1833-1840. DOI: 10.1063/1.1740588

- [15] Lee C, Yang W, Parr RG. Development of the colic-Salvetti correlation-energy formula into a functional of the electron density. *Physical Review B*. 1988;**98**:785-789. DOI: 10.1103/PhysRevB.37.785
- [16] Becke AD. A new mixing of Hartree-Fock and local density-functional theories. *Journal of Chemical Physics*. 1993;**98**:1372-1378. DOI: 10.1063/1.464304
- [17] Najafpour MM, Renger G, Holynska M, Moghaddam AN, Aro EM, Carpentier R, et al. Manganese compounds as water-oxidizing catalysts: From the natural water-oxidizing complex to Nanosized manganese oxide structures. *Chemical Reviews*. 2016;**116**:2886-2936. DOI: 10.1021/acs.chemrev.5b00340
- [18] Dexheimer SL, Klein MP. Detection of a paramagnetic intermediate in the S1 state of the photosynthetic oxygen-evolving complex. *Journal of American Chemical Society*. 1992;**114**:2821-2826. DOI: 10.1021/ja00034a010
- [19] Yamauchi T, Mino H, Matsukawa T, Kawamori A, Ono T. Parallel polarization electron paramagnetic resonance studies of the S1-state manganese cluster in the photosynthetic oxygen-evolving system. *Biochemistry*. 1997;**36**:7520-7526. DOI: 10.1021/bi962791g
- [20] Campbell KA, Gregor W, Pham DP, Peloquin JM, Debus RJ, Britt RD. The 23 and 17 kD extrinsic proteins of photosystem II modulate the magnetic properties of the S1-state manganese cluster. *Biochemistry*. 1998;**37**:5039-5045. DOI: 10.1021/bi9800552
- [21] Suga M, Akita F, Hirata K, Ueno G, Murakami H, Nakajima Y, et al. Native structure of photosystem II at 1.95 Å resolution viewed by femtosecond X-ray pulses. *Nature*. 2015;**517**:99-103. DOI: 10.1038/nature13991
- [22] Kusunoki M. S1-state Mn4Ca complex of photosystem II exists in equilibrium between the two most-stable isomeric substates: XRD and EXAFS evidences. *Journal of Photochemistry and Photobiology B*. 2011;**104**:100-1010. DOI: 10.1016/j.jphotobiol.2011.03.002
- [23] Bardeen J, Cooper LN, Schrieffer JR. Theory of superconductivity. *Physical Review*. 1957;**108**:1175-1204. DOI: 10.1103/PhysRev.108.1175
- [24] Schrieffer JR. *Theory of Superconductivity*. New York: WA Benjamin, Inc; 1964. pp. 1-282 ISBN: 9780429975332
- [25] Fröhlich H. Theory of the superconducting state. I. the ground zero of temperature. *Physical Review*. 1950;**79**:845-846. DOI: 10.1103/PhysRev.79.845
- [26] Bogoliubov NN. A new method in the theory of superconductivity. *Soviet Physics JETP*. 1958;**34**:41-46
- [27] Drozdov AP, Erements MI, Troyan IA, Ksenofontov V, Shylin SI. Conventional superconductivity at 203 kelvin at high pressures in the sulfur hydride system. *Nature*. 2015;**525**:73. DOI: 10.1038/nature14964